ELSEVIER

Carbohydrate Research 294 (1996) 1–13

CARBOHYDRATE
RESEARCH

Conformational analysis of asperlin by NMR spectroscopy and molecular modeling [1]

Emmanuel Mikros [a], Photis Dais [b,*], Françoise Sauriol [c]

[a] *Department of Pharmacy, Division of Pharmaceutical Chemistry, University of Athens, 15771 Athens, Greece*
[b] *Department of Chemistry, University of Crete, 71409 Iraklion, Crete, Greece*
[c] *Department of Chemistry, McGill University, Montreal, Quebec, Canada H3A 2A7*

Received 1 February 1996; accepted in revised form 1 August 1996

Abstract

NOESY experiments and computerised molecular modeling have been employed to examine the configuration and conformation of the epoxypropyl side chain of asperlin in benzene solution. The data support the conclusion that the oxirane ring in this molecule has the 6*S*,7*R* configuration. Moreover, the $^3J_{H\text{-}5,H\text{-}6}$ coupling constant about the C-5–C-6 bond has been calculated using an equation suitable for the H-5–C-5–C-6–H-6 segment. This value does not support a single conformation, but rather conformational averaging that provides good agreement between the theoretical and experimental parameters. © 1996 Elsevier Science Ltd.

Keywords: Asperlin; NOESY; Conformation; Molecular modeling

1. Introduction

The compound 5-acetoxy-5,6-dihydro-6-(1,2-epoxypropyl)-2-pyrone (**1**), isolated [1] from cultures of *Aspergillus nidulans* and termed *asperlin* has been shown to posses antibiotic and antitumor activity [2]. Earlier NMR spectroscopic [3–6], synthetic [3–8], and X-ray diffraction [9] studies of asperlin have demonstrated that the pyrone ring of **1** assumes a semi-planar conformation, that the 4,5-substituents of the lactone ring have the L-*threo* configuration, and that the exocyclic oxirane ring is *trans*. The two possible diastereomeric forms of **1** with respect to the configuration of the oxirane ring are 6*S*,7*R* (**1a**) and 6*R*,7*S* (**1b**). X-ray diffraction [9] and total synthesis [7,8] of the two

---

[*] Corresponding author.

[1] This paper is dedicated with much appreciation to Professor Arthur S. Perlin on the occasion of his 73rd birthday.

PII S0008-6215(96)00201-7

diastereomers have confirmed that the absolute configuration of the natural material is 6*S*,7*R*. On the other hand, ^{1}H non-selective and selective relaxation rates, together with NOE experiments for **1** in benzene-d_6 solutions, are consistent with the 6*R*,7*S* configuration [6]. However, the conclusions derived in the latter study are not consistent with the conformation of the epoxy ring of the natural asperlin for two main reasons. Firstly, the experimental inter-proton distances, H-4–H-7 and H-5–H-7, obtained from relaxation rates were compared with those calculated from stereo-models, which involve a high degree of inaccuracy (20–30%), especially for flexible molecules. Secondly, several orientations of the epoxypropyl ring about the C-5–C-6 bond should contribute to the measured ^{1}H relaxation rates and 1D NOE values. These conformations, corresponding to local and global minima in the conformational energy map, were not taken into consideration when determining inter-proton distances. Hence, there is no single energetically reasonable conformation that would fit the experimental data [10].

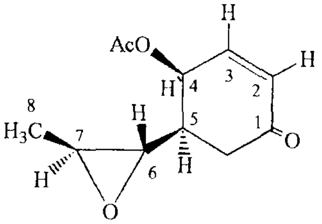

1

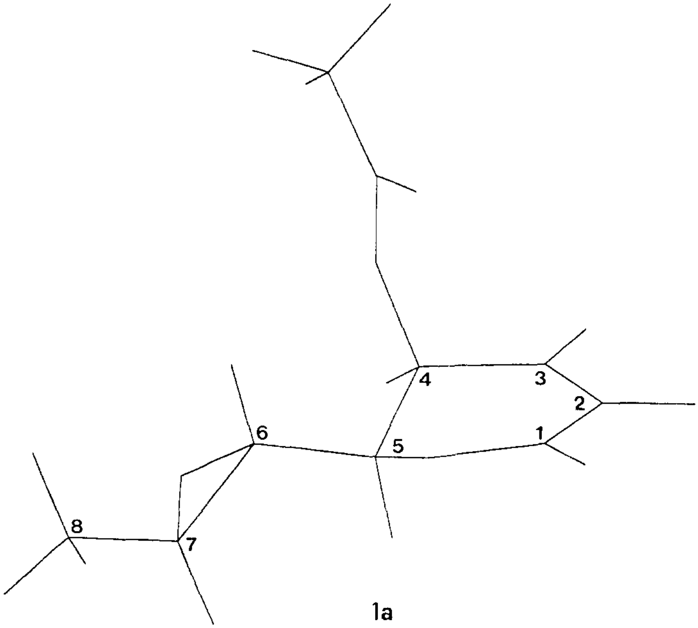

1a

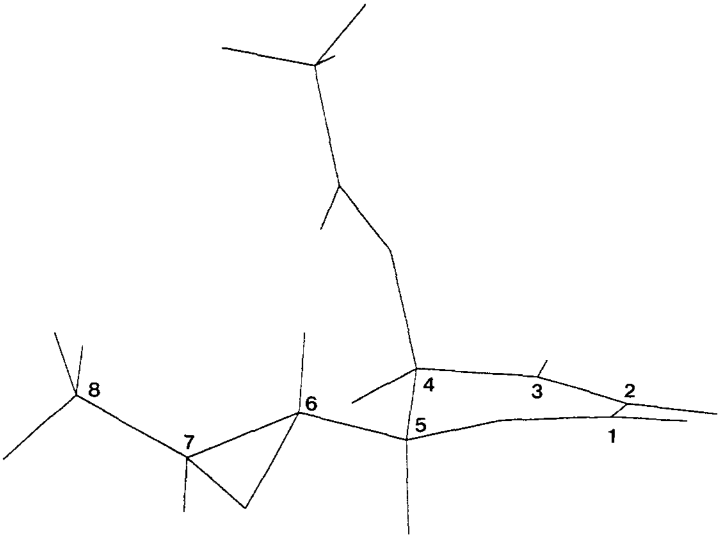

1b

The present study is an attempt to describe the configuration and conformation of the oxirane ring of **1** through phase-sensitive NOESY experiments and dynamic interpretation of the NMR data. In this procedure [11], theoretical 2D NOE spectra are calculated for a rapidly interchanging ensemble of structures, and compared with experimental 2D NOE intensities.

2. Experimental

NMR spectroscopy.—Phase-sensitive ^{1}H NOESY [12] experiments were conducted on a Bruker ARX spectrometer operating at 400 MHz for the proton nucleus. NOESY spectra were recorded with mixing times 2.0, 2.5, 3.0, 3.5, and 4.0 s. The recycling time was set to 15 s. A variable delay of 20 ms was introduced at the beginning of the mixing time in order to suppress *J*-peak transfer [13]. 256×512 data matrices were zero-filled to 512×512, and a $\pi/2$ shifted sine-squared weighting function was applied prior to Fourier transformation. NOESY cross-peak intensities were evaluated from the summed ω_1 subspectra contributing to a specific signal.

Selective 2DJ ^{13}C–^{1}H heteronuclear experiments [14] were conducted on a Varian XL-300 spectrometer operating at 75.4 and 300 MHz for the carbon and proton nuclei, respectively. The 180° selective pulse on proton resonances was calibrated by using a DANTE pulse-train [15] comprising 60 (hard) pulses of 2.5 μs each, separated by 3×10^{-4} s. Four transients were acquired for each of the 64 increments used to characterise the second domain of 16 Hz spectral width. The carbon signals were detected with 2048 data points. The 64×2048 matrices were pseudo-echo shaped and zero-filled prior to Fourier transformation.

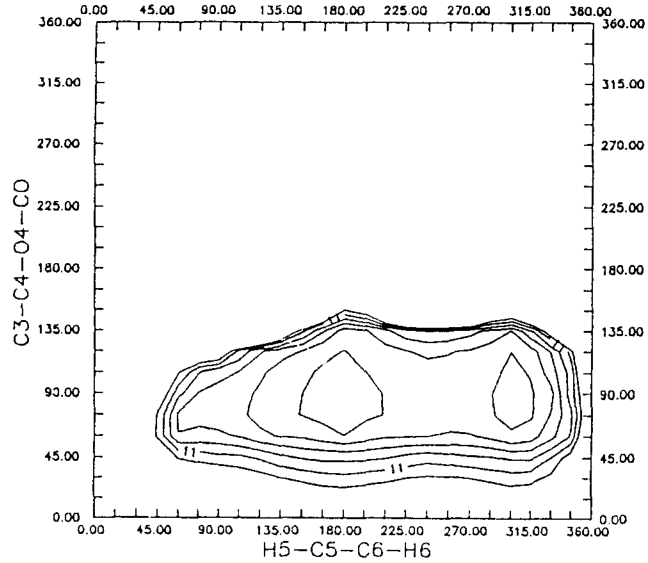

Fig. 1. Conformational energy map for the orientation of the acetyl substituent relative to the oxirane ring. The map was computed with the molecular mechanics MM$^+$ program at 20° of the H-5–C-5–C-6–H-6 and C-3–C-4–O-4–CO torsion angles.

Samples of 0.15 M and 0.5 M in benzene-d$_6$ were used for the NOESY and 2DJ heteronuclear experiments, respectively. The probe temperature was 30 ± 1° for both experiments.

Conformational analysis.—The initial geometry of *asperlin* was based on the atomic co-ordinates obtained from the crystal structure (conformer 6*S*,7*R*), and using the HyperChem software of Hypercube graphics to generate the geometry of the other conformer (6*R*,7*S*). Molecular geometry optimization and intramolecular energy calculations were performed using the AM1 molecular orbital program. Intramolecular energies for each structure were calculated upon rotation around the C-5–C-6 bond of **1**, scanning the whole angular range (360°) in 10° increments, while the epoxypropyl and pyrone rings were considered as rigid.

It should be noted that the AM1 method gave more accurate geometrical parameters than the MM$^+$ force field method. These parameters obtained from AM1 were closer to those observed in the crystal structure of asperlin from X-ray diffraction studies [9]. However, no difference in the energy profile upon rotation about the C-5–C-6 bond was observed by using either methods.

In order to set the relative orientation of the acetyl group, the conformational energy map in terms of the dihedral angles H-5–C-5–C-6–H-6 = $\Phi°$, and C-3–C-4–O-4–CO = $\Psi°$ was computed with the MM$^+$ force field program at 20° increments of Φ and Ψ torsion angles (Fig. 1). MM$^+$ calculations were performed without taking into account solute–solvent interactions, whereas for the electrostatic interactions the bond-dipole option of the program was used. Energy minimization was carried out using the

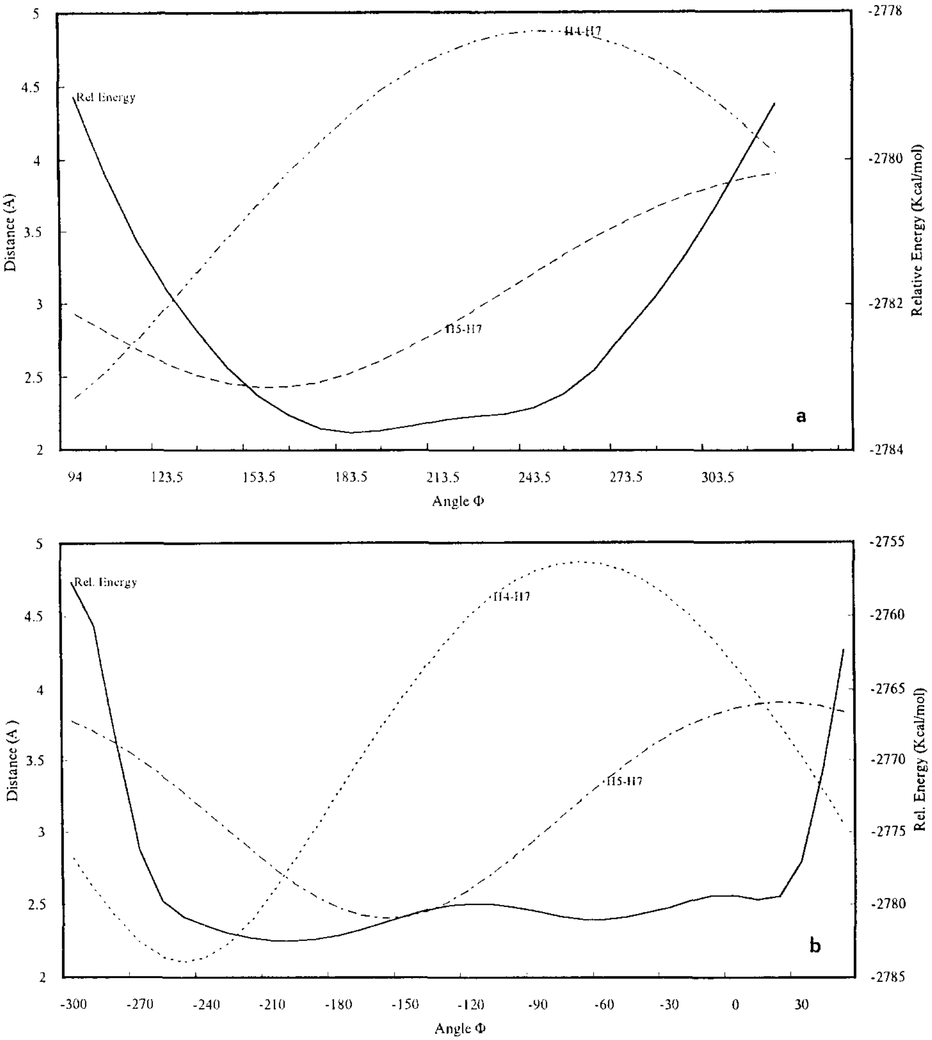

Fig. 2. Calculated relative energy (in kcal mol^{-1}) of *asperlin*; H-4–H-7; H-5–H-7 interproton distances as a function of the torsion angle Φ about the C-5–C-6 bond. Only the regions of the low-energy conformers for the (a) 6*S*,7*R*, and (b) 6*R*,7*S* configurations are shown.

Pollack–Ribiere method, which was included in the geometry optimization procedure of the HyperChem software. Minimization was executed to a convergence gradient of 0.01.

The orientation of the acetyl substituent is identified by the angle $\Psi \sim 80°$, corresponding to the low-energy conformer in the map (Fig. 1). This orientation was fixed for the energy calculations of the various conformers generated upon rotation about the C-5–C-6 bond. Fig. 2 shows the potential energy profile versus the torsion angle, Φ, around the C-5–C-6 bond for each conformer **1a** and **1b**. The range of torsion angles shown in this figure correspond to the energy minima for each conformer.

Calculations of coupling constants and the relaxation matrix.—The generated structures from conformational analysis were used for the calculation of the theoretical value of the vicinal coupling constant, ${}^3J_{\mathrm{H\text{-}5,H\text{-}6}}$, for each different conformation, namely,

$$^3J_{\mathrm{H,H}} = 4.228\cos 2\Phi - 0.910\cos\Phi + 4.971$$

for the 6*S*,7*R* conformation

and

$$^3J_{\mathrm{H,H}} = 4.228\cos 2\Phi - 0.910\cos\Phi - 1.624\sin 2\Phi + 4.971$$

for the 6*R*,7*S* conformation

These Karplus-type equations were obtained from the general relationship of the *J*-dependence on the dihedral angle, Φ, proposed by Haasnoot et al. [16] using simple trigonometric identities [see Eqs. (8) and (9) of this reference]. The different functional forms of the above equations used for the two conformers is attributed to the different orientations of the substituents at α and β positions relative to the coupled protons, which influence the *J* coupling [16]. It appears that the relative orientations of the oxygen of the oxirane ring and the methyl substituent with respect to the H-5 and H-6 coupled protons are different for the 6*S*,7*R* and 6*R*,7*S* conformers.

The calculation of the macroscopic coupling constant requires consideration of the balanced contribution from each conformation in the form of an ensemble average, that is

$$\langle {}^3J_{\mathrm{H,H}} \rangle = \sum_n P_i {}^3J_{i\mathrm{H,H}}$$

where P_i represents the relative population of the *i*-th conformer with energy, E_i, and is governed by a Boltzmann distribution,

$$P_i = \exp(-E_i/kT) \Big/ \sum_n \exp(-E_i/kT).$$

Averaging of the coupling constant was performed on the total population of 35 conformers for each structure **1a** and/or **1b**.

The theoretical NOESY spectrum was computed using the new form of the MARDIGRAS and CORMA programs [17], which have been modified [11,18] to incorporate (1) internal motions modeled by a model-free approach, (2) chemical exchange described by a kinetic matrix of exchange rates, and (3) quality factors *R* and R^x, which reflect the match of experimental and calculated NOESY peak intensities. The *R* factor is equivalent to the crystallographic *R*-factor, and R^x is a variation of the *R* factor involving sixth-root weighting of intensities to avoid domination by short relaxation pathways, that is,

$$R^x = \sum_i |I_e^{1/6}(i) - I_c^{1/6}(i)| \Big/ \sum_i |I_e^{1/6}(i)|$$

where $I_e(i)$ is the experimental and $I_c(i)$ is the corresponding calculated intensity of the cross peak *i* for a particular structure [11,17,18]. In this procedure, the *R* and R^x factors are calculated for a rapidly interchanging ensemble of structures, the relaxation rates of individual snapshots are averaged, and the resulting theoretical intensity matrix is compared with experimental intensities. This is distinct from arithmetically comparing averaged intensities for a set of structures [11]. Only the conformations with values of relative energy within a range of 5 kcal/mol were taken into account in the averaging procedure of this study.

The simulation of NOESY intensities with the CORMA program is based on the ensemble averaged relaxation rates over the number of conformers resulting from the conformational analysis. The same Boltzmann factor, used for the calculations of the theoretical J couplings, was applied for averaging of dipolar relaxation rates. Structures having a relative population less than 0.1% were not taken into account in the present calculations.

3. Results and discussion

1D NMR data.—Table 1 summarises the ^1H and ^{13}C chemical shifts, as well as the proton–proton and carbon–proton coupling constants. The ^{13}C–^1H coupling constants were obtained in this study from selective 2DJ experiments. These NMR parameters are in accordance with the previous [3–6] interpretation of the stereochemistry of **1**. However, ambiguity arises as far as the conformation of the pyrone ring is concerned. In the 6*S*,7*R* configuration, the 5-oxirane substituent may be pseudo-equatorial (**1a**) or pseudo-axial (**2a**). Quantum-mechanical (AM1) and force field (MM$^+$) calculations showed that the two forms differ very little in energy (see Fig. 2). This fact is not surprising, since in these forms the ring-substituent interactions are between C-6 and OAc, both of which are *gauche*, as shown by the conformational energy map in Fig. 1. Consequently, forms **1a** and **2a** are expected to be about equally stable. Nevertheless, coupling constant data appear mainly to support form **1a**. Thus, no ^3J coupling is

Table 1
Proton and carbon-13 nuclear magnetic resonance data for *asperlin* [a]

Proton	$\delta\ ^1H$ [b]	$^3J_{H,H}$ [c]	Carbon	$\delta\ ^{13}C$ [b]	$^2J_{C,H}$ [c,d]	$^3J_{C,H}$ [c,d]
			C-1	161.1	$J_{C\text{-}1,H\text{-}2} = 4.2$	$J_{C\text{-}4,H\text{-}2} = 8.8$
H-2	5.71	$J_{H\text{-}2,H\text{-}3} = 9.7$	C-2	124.8	$J_{C\text{-}2,H\text{-}3} = 1.5$	$J_{C\text{-}1,H\text{-}3} = 12.1$
H-3	6.30	$J_{H\text{-}3,H\text{-}4} = 5.7$	C-3	140.4	$J_{C\text{-}4,H\text{-}3} = 3.6$	$J_{C\text{-}5,H\text{-}3} = 4.7$
H-4	4.87	$J_{H\text{-}4,H\text{-}5} = 2.8$	C-4	62.2	$J_{C\text{-}3,H\text{-}4} = 5.1$	$J_{CO,H\text{-}4} = 3.2$
H-5	3.40	$J_{H\text{-}5,H\text{-}6} = 6.9$	C-5	78.4	$J_{C\text{-}5,H\text{-}4} = 1.6$	$J_{C\text{-}2,H\text{-}4} = 5.1$
H-6	2.79	$J_{H\text{-}6,H\text{-}7} = 2.0$	C-6	55.1	$J_{C\text{-}4,H\text{-}5} = 4.2$	$J_{C\text{-}1,H\text{-}5} = 0.9$
H-7	2.58	$J_{H\text{-}7,H\text{-}8} = 5.2$	C-7	53.8	$J_{C\text{-}6,H\text{-}5} = 6.3$	$J_{C\text{-}3,H\text{-}5} = 1.0$
H-8	0.93	–	C-8	16.9	$J_{C\text{-}5,H\text{-}6} = 5.4$	$J_{C\text{-}7,H\text{-}5} = 3.9$
					$J_{C\text{-}7,H\text{-}6} = 1.8$	$J_{C\text{-}4,H\text{-}6} = 1.7$
					$J_{C\text{-}6,H\text{-}7} = 1.8$	$J_{Me,H\text{-}6} = 2.0$
					$J_{Me,H\text{-}7} = 6.4$	$J_{C\text{-}5,H\text{-}7} = 2.0$

[a] The chemical shifts for the acetyl group are not shown.

[b] In ppm relative to TMS.

[c] Coupling constants in Hz.

[d] Less accurate $^4J_{C,H}$ coupling constants between C-6, H-3 and C-1, H-4 pairs have been observed.

detected between C-6 and H-4, and only a small coupling between C-3 and H-5 (1.0 Hz) is observed (Table 1). These values are consistent with dihedral angles of about 90° and 60° for the C-3–C-4–C-5–H-5 and the C-6–C-5–C-4–H-4 fragments, respectively. If the side-chain were axial, as in **2a**, two large couplings (~ 5–6 Hz) should have been observed. Additional evidence for the prominence of form **1a** comes from the experimental proton–proton coupling constant data in Table 1. As noted by Lesage et al. [4], the lack of long-range coupling between H-2 and H-4, as well as the values of 5.7 and 2.8 Hz for $^3J_{\text{H-3,H-4}}$, and $^3J_{\text{H-4,H-5}}$, respectively, favour a conformation in which the C-4–H-4 bond approaches coplanarity with the olefinic bond of the pyrone ring, and that the 4-acetoxyl group is in a *trans* diaxial relationship with respect to H-5. A third piece of evidence to support the assertion that the **1a** form is predominant comes from the calculation of $^3J_{\text{H-3,H-4}}$ through the Karplus equation as modified by Garbish et al., [19] and Abraham et al. [20] For H-4–C-4–C-3–H-3 dihedral angles of 39° (for **1a**), and 81° (for **2a**), obtained from energy minimisation procedures (see experimental), the former equation gives $^3J_{\text{H-3,H-4}}$ values of 5.0 and 2.7 Hz, respectively, whereas the latter equation gives values of 5.3 and 0 Hz for **1a** and **2a**, respectively. These values are to be compared with the experimental value of 5.7 Hz. A similar comparison can be made between the experimental coupling constant between H-4 and H-5 protons (2.8 Hz) and those calculated for the two conformers through the Karplus equation [16]:

$$^3J_{\text{H-4,H-5}} = 3.948\cos 2\Theta - 0.910\cos\Theta - 1.624\sin 2\Theta + 4.812$$

The calculated values are: for **1a**, $\Theta = 49°$, $J = 2.1$ Hz; for **2a**, $\Theta = -40°$, $J = 6.4$ Hz. It should noted that asperlin has the form **1a** in the solid [9].

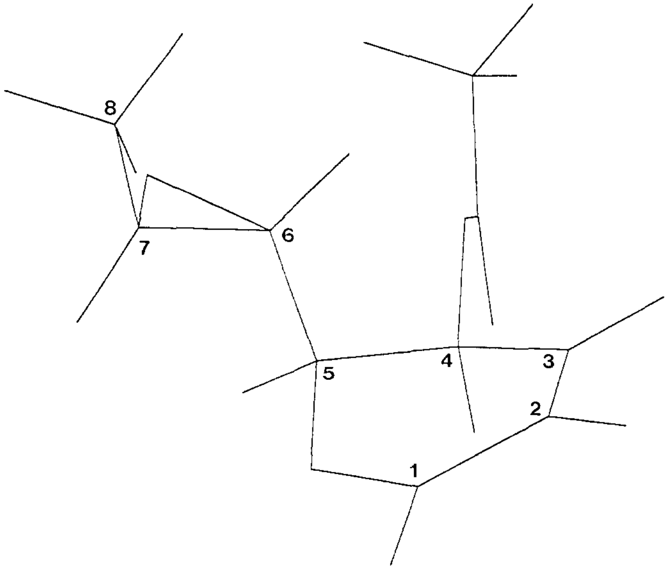

2a

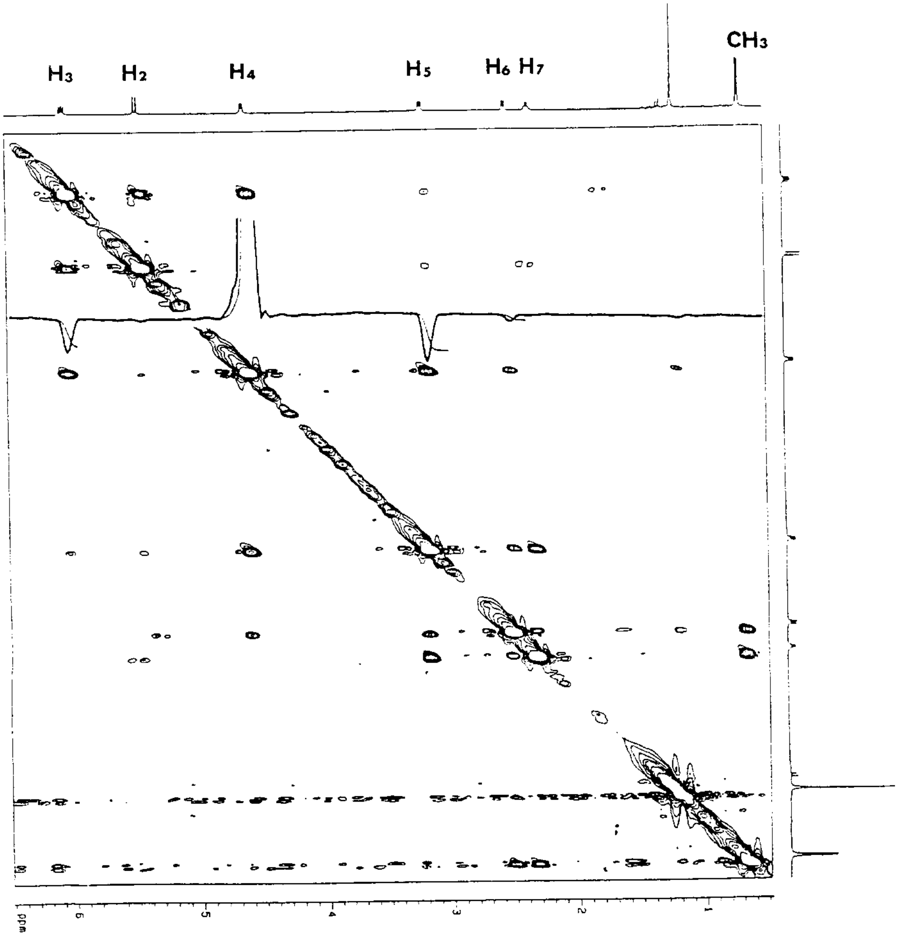

Fig. 3. Unsymmetrized, phase-sensitive 400-MHz ^{1}H NOESY spectrum of *asperlin* in benzene. The spectrum was obtained with mixing time of 2.5 s at 303 K.

NOESY intensities.—Fig. 3 illustrates the experimental 400-MHz NOESY spectrum of **1** in benzene-d_6 solution with a mixing time of 2.5 s. The theoretical spectrum (not shown) was calculated assuming that the epoxypropyl ring adopts the (6*S*,7*R*) (**1a**) and (6*R*,7*S*) (**1b**) configurations, respectively, and that the acetyl substituent is pseudo-axial in both forms. The experimental spectrum (Fig. 3) shows several cross-peaks between protons in the same pyrone or epoxypropyl residue, and more interestingly between interesidue protons. In particular, cross-peaks of various intensities connect the pairs H-5, H-6; H-5, H-7; and H-4, H-6. No cross-peak appears between the H-4 and H-7 protons in this spectrum, as well as in the spectra obtained with different mixing times. The theoretical NOESY spectra, with a mixing time of 2.5 s, of both isomers are similar to the experimental one except for the fact that the cross-peak connecting the H-4 and H-7 is not observed in the spectrum of **1a**, whereas such an off-diagonal peak appears in the spectrum calculated for the **1b** form. This is strong evidence that the epoxypropyl ring in the natural *asperlin* adopts the 6*S*,7*R* configuration in conformity with other suggestions [7–9].

The reason for the difference, which appears in all the theoretical spectra calculated with different mixing times, can be seen in Fig. 2, where the various interesidue proton distances are plotted as a function of the torsion angle Φ about the C-5–C-6 bond. A larger number of conformers with smaller H-4–H-7 distances (up to 2.1 Å) contribute to the NOE of these protons in the **1b** form than in the **1a** form, a fact which is reflected in their corresponding calculated NOESY spectra. It is interesting to mention at this stage the values of the H-4–H-7 and H-5–H-7 distances calculated [5] from mono-selective proton relaxation rates and NOE values, and from a combination of mono- and biselective proton relaxation rates. The range of these values was 2.79–2.92 Å for the H-4–H-7 distance, and 2.73–2.88 Å for the H-5–H-7 distance (with an average propagated error of ±0.10 Å). No discrimination can be made between forms **1a** and **1b** on the basis of these interproton distances, which cover a small fraction of the total conformational space (see Fig. 2).

Experimental and calculated NOESY intensities a_{ij} for the **1a** form (mixing time 2.5 s) are collected in Table 2. The experimental intensities were normalised by the program with respect to the calculated absolute values. The normalization was performed over a fixed distance, that is, by using a normalization factor obtained from the experimental cross-peak intensity of two protons at a fixed distance. The experimental intensity of the H-2 and H-3 protons, which are located in the rigid part of the pyrone ring, and hence correspond to a fixed distance, was used in the normalization. This normalization procedure over a fixed distance was preferred over other choices in CORMA, because it provides an opportunity to test the validity of the calculated intensities between other pairs of protons at fixed distances. From Table 2, it can be seen that the normalised experimental intensities of pairs of protons H-6–H-7, H-4–H-5, and H-3–H-4 are in good agreement with the theoretical values, indicating that the calculations are fairly reliable.

The match of theoretical to experimental data reflected by the residual indices $R = 0.211$ (0.202) and $R^x = 0.043$ (0.044) is quite satisfactory regarding the experimental error (~ 20%) involved in the determination of the a_{ij} intensities. For the remaining calculated intensities of the **1a** and **1b** forms with different mixing times (2.0, 2.5, 3.0, 3.5, and 4.0 s), the R factors range from 0.211 to 0.344, and the R^x factor from 0.043 to 0.090.

Overall and internal motions.—One of the major difficulties in reproducing the theoretical NOESY intensities for flexible molecules, using the complete relaxation matrix analysis (CORMA), is the evaluation of the relative rates of overall and internal motions. Usually, molecular correlation times describing the various modes of reorientation can be obtained from ^{13}C NMR spin-lattice relaxation times (under the extreme narrowing condition) in combination with dynamic models [21]. Such a treatment has been undertaken for *asperlin* [6]. The rigidity of the pyrone ring and its semi-planar conformation result in an overall ellipsoidal shape. The pyrone carbons are relaxed predominantly via the overall motion, which can be adequately approximated by the diffusion of a prolate ellipsoid with the major axis passing through the C-2–H-2 bond.

Table 2
Experimental, normalised experimental (in parentheses) and theoretical (in brackets) cross-peak intensities for the 6*S*,7*R* and 6*R*,7*S* conformers of *asperlin*

	6*S*,7*R* conformer [a]							6*R*,7*S* conformer [b]						
	H-2	H-3	H-4	H-5	H-6	H-7	H-8	H-2	H-3	H-4	H-5	H-6	H-7	H-8
H-2	3.132			−0.006 (−0.002) [−0.002]				3.132	−0.006 (−0.002) [−0.003]					
H-3	−0.117 (−0.046) [−0.046]	2.324	−0.099 (−0.039) [−0.050]	−0.008 (−0.003) [−0.003]				−0.117 (−0.046) [−0.046]	2.324	−0.099 (−0.039) [−0.049]	−0.008 (−0.003) [−0.002]			
H-4			2.489	−0.135 (−0.053) [−0.057]	−0.021 (−0.008) [−0.011]	−0.000 (−0.000) [−0.000]				2.489	−0.135 (−0.053) [−0.054]	−0.021 (−0.008) [−0.009]	0.000 (0.000) [−0.0027]	
H-5				2.511	−0.037 (−0.014) [−0.011]	−0.086 (−0.034) [−0.025]					2.511	−0.037 (−0.015) [−0.012]	−0.086 (−0.034) [−0.023]	
H-6					2.520	−0.040 (−0.016) [−0.011]	−0.057 (−0.022) [−0.013]					2.520	−0.040 (−0.016) [−0.010]	−0.057 (−0.022) [−0.013]
H-7						2.205	−0.082 (−0.032) [−0.022]						2.205	−0.082 (−0.032) [−0.022]
H-8							4.366							4.366

[a] RMS1 (the absolute root mean square error) = 0.0065; RMS2 (the relative root mean square error) = 0.28; $R = 0.211$; $R^x = 0.043$; Average error = 0.0014.
[b] RMS1 = 0.0067; RMS2 = 0.271; $R = 0.202$; $R^x = 0.044$; Average error = 0.0027.

The correlation times describing the anisotropic motion parallel and perpendicular to the major axis of the ellipsoid were found to be $\tau_{\parallel} = 3.7 \times 10^{-11}$ s, and $\tau_{\perp} = 5.2 \times 10^{-11}$ s, respectively, at 303 K. The correlation time for the epoxypropyl ring has been evaluated ($\tau_e = 2.0 \times 10^{-11}$ s at 303 K) assuming internal motion of restricted amplitude, whereas that of the epoxymethyl substituent has been evaluated ($\tau_i = 2.6 \times 10^{-12}$ s at 303 K) by applying the stochastic diffusion model of multiple internal rotations. However, the previously mentioned dynamic models used to describe the overall and internal motions of *asperlin* cannot be incorporated into the CORMA program without serious modifications. This program calculates spectral densities in the form of the free-model approach [22], $J(\omega, A, S^2, \tau_1, \tau_2, \tau_e)$, as a function frequency, ω, the anisotropy parameter, A, the order parameter, S^2, the overall correlation times, τ_1 and τ_2, and the internal correlation time, τ_e. In the program the ratio τ_1/τ_2 is used. For $\tau_1/\tau_2 = 1$, or $A = 1$, isotropic overall motion is obtained. If the order parameter S^2 is set to 1, the internal motion is ignored. If both A and S^2 are set to one, isotropic motion with no internal rotation is considered. Furthermore, methyl internal rotation is modeled by CORMA with 3 or 18 sites jumps. In view of these difficulties, we calculated the parameters A and S^2 for the overall and internal motions using the spectral density of the model-free approach and keeping $\tau_1 = \tau_{\parallel} = 3.7 \times 10^{-11}$ s, $\tau_2 = \tau_{\perp} = 5.2 \times 10^{-11}$ s, and $\tau_e = 2.0 \times 10^{-11}$ s. The input parameters for CORMA regarding rates of motion were $\tau_1/\tau_2 = 0.71$, $A = 0.68$, $S^2 = 0.614$, and the value of τ_e. Also, calculations were performed assuming isotropic overall motion ($A = 1$, $S^2 = 0.675$), and/or no internal rotation ($A = 1$, $S^2 = 1$). In both cases, the results of the AM1 simulation were mediocre.

At this stage, it is worth discussing the validity of the model-free approach, which has been used to describe the dynamics of *asperlin*. According to Lipari and Szabo [22], this approach is accurate when (1) the internal motions are much faster than the overall motion, and (2) they occur within the extreme narrowing region. Although the second rule of the model-free theory applies to the internal rotation of the epoxypropyl ring, the first rule, which implies the decoupling of the overall and internal motions, does not. As a matter of fact, the internal motion of the oxirane ring is slightly faster than the overall motion ($\tau_e/\tau_{\parallel} = 0.5$, $\tau_e/\tau_{\perp} = 0.4$). Nevertheless, the model-free approach is an exact method for the evaluation of the parameters, S^2 and τ_e, with no restriction on the relative magnitude of the correlation times of the overall and internal rotation provided that $S^2 > 0.3$ [22]. Since, for the present study, $S^2 = 0.614$, we do not expect any considerable influence on the calculated NOESY intensities by using the model-free approach for describing the dynamics of the oxirane ring of *asperlin*. To estimate the range of the figures presented in Table 2, we performed the entire set of calculations using the same values of $\tau_1 = \tau_{\parallel}$, $\tau_2 = \tau_{\perp}$, and S^2 as above, but using a slower ($\tau_e = 2.0 \times 10^{-10}$ s) and a faster ($\tau_e = 2.0 \times 10^{-12}$ s) internal motion for the oxirane ring relative to the overall molecular tumbling. In both cases, the calculated cross-peak intensities were similar to those calculated with $\tau_e = 2.0 \times 10^{-11}$ s, to within 6% or better. In particular, the maximum deviation for the crucial H-4–H-7 cross-peak intensity was 3%. Kumar et al., [23] have arrived at the same conclusion, that is, only very low values of S^2 affect the interproton distances, introducing internal motions in the simulation of the 2D NOE spectra of the protein bovine pancreatic trypsin inhibitor

(BPTI). From the average order parameter $S^2 = 0.8$ and correlation time $\tau_e = 2.0 \times 10^{-10}$ s, the error in the interproton distances, which did not involve the exceptional residue gly^{28}, was found to be negligible. For the residue gly^{28}, for which the order parameter was as low as 0.2, the largest deviation for the gly^{28}NH–gly^{28}C$^{\alpha 2}$H proton pair was 0.62 Å [23].

Comparison of the NMR and molecular mechanics coupling constants data.—The value of the coupling constant, $^3J_{\text{H-5,H-6}} = 6.7$ Hz, about the C-5–C-6 bond has been calculated for the Boltzmann distribution of the 35 conformers as described in the experimental section. This value calculated for the average structure of **1a** compares favourably with the experimental value of 6.9 Hz (Table 1).

Acknowledgements

The authors have benefitted from discussions with Professor Arthur S. Perlin from McGill University.

References

[1] A.D. Argoudelis and J.F. Zieserl, *Tetrahedron Lett.*, (1966) 1969–1973.

[2] A.D. Argoudelis, J.H. Coats, and R.R. Herr, *Antimicrob. Agents Chemother.*, (1965) 801–803.

[3] S. Lesage and A.S. Perlin, *Can. J. Chem.*, 56 (1978) 3117–3120.

[4] S. Lesage and A.S. Perlin, *Can. J. Chem.*, 56 (1978) 2889–2896.

[5] P. Dais and A.S. Perlin, *Can. J. Chem.*, 63 (1985) 1009–1012.

[6] P. Dais and G. Fainos, *Can J. Chem.*, 64, (1986) 560–565.

[7] S. Valverde, B. Herradon, R.M. Rabanal, and M. Martin-Lomas, *Can. J. Chem.*, 65 (1987) 339–342.

[8] T.K. Shing and M. Alout, *Can. J. Chem.*, 68 (1990) 1035–1037.

[9] (a) K. Fukuyama, Y. Katsube, and A. Noda, *Bull. Chem. Soc. Jpn.*, 51 (1978) 3175–3181; (b) S. Ramesh and R.W. Frank, *Tetrahedron: Assymetry*, 1 (1990) 137–140.

[10] C. Meyer, S. Perez, C. Herve du Penhoat, and V. Michon, *J. Am. Chem. Soc.*, 115 (1993) 10300–10310.

[11] U. Schmitz, A. Kumar, and T.L. James, *J. Am. Chem. Soc.*, 114 (1992) 10654–10656.

[12] S. Macura, Y. Huang, D. Suter, and R.R. Ernst, *J. Magn. Reson.*, 43 (1981) 259–281.

[13] D. Neuhaus and M. Williamson, *The Nuclear Overhauser Effect in Structural and Conformational Analysis*, VCH Publishers, Cambridge, 1989, p 292.

[14] A. Bax and R. Freeman, *J. Am. Chem. Soc.*, 104 (1982) 1099–1100.

[15] G. Bodenhausen, R. Freeman, and G.A. Morris, *J. Magn. Reson.*, 23 (1976) 171–175.

[16] C.A.G. Haasnoot, F.A.A.M. de Leeuw, and C. Altona, *Tetrahedron.*, 36 (1980) 2783–2792.

[17] (a) J.W. Keepers and T.L. James, *J. Magnetic Reson.*, 57 (1984) 404–426; (b) B.A. Borgias and T.L. James, *J. Magn. Reson.*, 79 (1988) 493–512.

[18] B.A. Borgias and T.L. James, *J. Magn. Reson.*, 87 (1990) 475–487; MARDIGRAS program, University of California, 1990.

[19] E.W. Garbish, *J. Am. Chem. Soc.*, 86 (1964) 5561–5564.

[20] R.J. Abraham, M.A. Cooper, J.R. Salman, and P. Whittaker, *Org. Magn. Reson.*, 4 (1972) 489–493.

[21] P. Dais, Adv. *Carbohydr. Chem. Biochem.*, 51 (1995) 63–131.

[22] G. Lipari and A. Szabo, *J. Am. Chem. Soc.*, 104 (1982) 4546–4559; *ibid*, 104 (1982) 4559–4570.

[23] A. Kumar, T.L. James, and G.C. Levy, *Israel J. Chem.*, 32 (1992) 257–261.